Journal of Catalysis **184,** 144–156 (1999)
Article ID jcat.1999.2434, available online at http://www.idealibrary.com on IDEAL®

In Situ Infrared Study of Methanol Synthesis from CO_2/H_2 on Titania and Zirconia Promoted Cu/SiO_2

Tobin C. Schilke, Ian A. Fisher, and Alexis T. Bell

Chemical Sciences Division, Lawrence Berkeley National Laboratory and Department of Chemical Engineering, University of California, Berkeley, California 94720

Received September 30, 1998; revised January 20, 1999; accepted January 22, 1999

***In situ* infrared studies of methanol synthesis from H_2/CO_2 have been conducted over Cu/SiO_2 promoted with ZrO_2, TiO_2, and a mixture of TiO_2/ZrO_2, with the aim of establishing the means by which the added oxide influences the activity of the catalyst for methanol synthesis. While ZrO_2 and TiO_2 individually enhance the methanol synthesis activity of Cu/SiO_2, a significantly greater enhancement is achieved by addition of both oxides simultaneously. In the absence of oxide addition, infrared spectra taken under reaction conditions suggest that methanol synthesis from CO_2 takes place on the surface of Cu exclusively. When ZrO_2 is added to the catalyst, there is strong evidence for methanol synthesis on the surface of both Cu and ZrO_2. Catalysis on the surface of ZrO_2 occurs as a consequence of CO_2 adsorption to form *b*–HCO_3–Zr, which then undergoes progressive hydrogenation to form methanol. The required atomic hydrogen is supplied from the surface of Cu particles by spillover. When TiO_2 is added there is no evidence for catalysis occurring on the oxide surface, but strong evidence for an enhancement in the level of reaction occurring on the surface of Cu. The observed increase in the rate of methanol synthesis is attributed to a reconstruction of the Cu particles to expose the (100) surface, which have been demonstrated to be significantly more active than the (110) or (111) surfaces. The infrared spectra observed when a mixture of ZrO_2 and TiO_2 is added to Cu/SiO_2 resembles a composite of the spectra observed upon addition of the individual oxides, and hence, the enhanced rate of methanol synthesis is ascribed to the combined effects of ZrO_2 and TiO_2.**

INTRODUCTION

Due to the increasing consumption of methanol for fuel applications, significant research has been undertaken to study the catalytic synthesis from hydrogen and carbon dioxide using supported copper catalysts (1). Many authors have shown that for Cu catalysts the support or promoter can significantly affect the activity for methanol synthesis (2–4). Zirconia and titania have emerged as particularly interesting support materials as they enhance the activity of Cu for methanol synthesis from CO_2/H_2 (3, 5–18). It has also been demonstrated recently that silica-supported Cu promoted ZrO_2 and TiO_2 is more active than silica-supported Cu promoted with ZrO_2 or TiO_2 alone (18).

A bifunctional mechanism has been proposed to explain the high activity of Cu/ZrO_2 and ZrO_2 promoted Cu/SiO_2 for methanol synthesis from CO_2 and H_2 (16). *In situ* infrared investigations of Cu/ZrO_2 indicate that ZrO_2 is more effective than Cu for the adsorption of CO_2 and that the synthesis of methanol occurs on the surface of ZrO_2, with hydrogen supplied by spillover from Cu (16). Less extensive *in situ* infrared and activity studies of Cu/TiO_2 and $Cu/ZrO_2/TiO_2$ catalysts seek to ascribe enhancement in activity to acid–base interactions of CO_2 with the metal oxide component (14, 17, 18). In the case of Cu/SiO_2 promoted with both ZrO_2 and TiO_2 it has been proposed that the superior activity of these catalysts relative to either ZrO_2 or TiO_2 promoted Cu/SiO_2 is due to the enhanced basicity of the promoter resulting from the formation of a mixed metal oxide. The present investigation was undertaken to gain further insight into how TiO_2 and ZrO_2/TiO_2 enhance methanol synthesis on Cu and in particular to verify the validity of the hypothesis that the addition of TiO_2 to ZrO_2 results in a more basic oxide. With these objectives in mind, *in situ* infrared studies were conducted of CO_2 adsorption and desorption, and methanol synthesis from CO_2 and H_2 on SiO_2 and Cu/SiO_2 promoted with ZrO_2, TiO_2, and a mixture of ZrO_2 and TiO_2.

EXPERIMENTAL

First, 5 wt% Cu/SiO_2 was prepared by the decomposition of $Cu(NO_3)_2$. The Cu/SiO_2 was promoted with TiO_2 and ZrO_2 by the hydrolysis of their respective isopropoxides. Details of the preparative procedure may be found in Ref. (19). Mixtures of TiO_2 and ZrO_2 were dispersed on SiO_2 in the same manner used to disperse these mixtures on Cu/SiO_2 (19). The Cu, Zr, and Ti contents of the catalysts were determined by ICP analysis. The compositions of all catalysts used in this study are listed in Table 1.

Bay Airgas UHP H_2, He, and CO_2 were purified prior to use. Hydrogen was passed through a Deoxo unit (Engelhard) to remove O_2 impurities by forming water which was subsequently removed by a molecular sieve trap (3A Davidson grade 564). He was passed through an

0021-9517/99 $30.00

TABLE 1

Compositions of Catalysts Used in This Study

Catalyst designation	Cu loding (wt%)	ZrO_2 loading (wt%)	TiO_2 loading (wt%)	Proportion of ZrO_2 to TiO_2 (wt%)	Cu area after reduction (m^2/g)	Cu area after reaction and re-reduction (m^2/g)
Cu(0)Zr(5)Ti(0)	0.0	5.0	0.0	100	—	—
Cu(0)Zr(2.5)Ti(2.5)	0.0	2.5	2.5	50	—	—
Cu(0)Zr(0)Ti(5)	0.0	0.0	5.0	0	0.00	—
Cu(5)Zr(0)Ti(0)	5.2	0.0	0.0	NA	0.68	0.63
Cu(5)Zr(5)Ti(0)	5.2	5.0	0.0	100	0.61	0.53
Cu(5)Zr(2.5)Ti(2.5)	5.2	2.5	2.5	50	0.58	0.60
Cu(5)Zr(0)Ti(5)	5.2	0.0	5.0	0	0.55	0.66
Cu(5)Zr(0)Ti(30)	5.2	0.0	30.0	0	—	—

oxysorb (CrO_2) trap to remove O_2 and then a molecular sieve trap. CO_2 was passed through a hopcalite trap (80% $MnO_2 + 20\%$ CuO) to remove CO and a molecular sieve trap to remove water. Purified gases were delivered to the infrared cell via Tylan Model FC-280 mass flow controllers. H_2O–H_2 mixtures were created by flowing H_2 (Bay Airgas) through a glass bubbler containing deionized water at 0.17 MPa and 295 K. This mixture was metered with a needle valve and delivered to the reactor via a bypass loop to prevent the water from contaminating the upstream lines.

In situ transmission infrared spectroscopy was performed using a 2-cm diameter catalyst disk of 0.2-mm thickness, weighing approximately 60 mg. The catalyst disk was contained in a low dead-volume infrared cell (19). Infrared spectra were collected using a Nicolet Magna 750 series II FTIR spectrometer equipped with a narrow band MCT detector. *In situ* absorbance spectra were obtained by collecting 64 scans at 4 cm^{-1} resolution. Each spectrum was referenced to a spectrum of the sample collected at the same temperature under He or H_2 flow as appropriate. Electrical resistance heaters heated the cell and an Omega Series CN-2010 programmable temperature controller controlled the cell temperature.

Prior to each experiment with a fresh sample of catalyst, the catalyst was reduced in $10\%H_2$/He flowing at 60 cm^3 (STP)/min. The reduction temperature was raised at 2 K/min from ambient to 523 K, after which the catalyst was further reduced at 523 K for >8 h in pure H_2 flowing at 40 cm^3 (STP)/min. Subsequent reductions were all performed at 523 K, but varied in time (always >8 h) to ensure that all observable surface species were removed.

The Cu surface area was measured by N_2O titration. Titrations were carried out in a stainless steel microreactor (7.7 mm ID) heated by a small furnace. Catalyst samples weighing 0.20 g were reduced via the procedure described above. A type K thermocouple in the center of the catalyst bed was connected to an Omega series CN-2010 programmable temperature controller for temperature measurement and control. He was passed through an oxysorb (CrO_2) trap to remove O_2 and then a molecular sieve trap. Purified gases were delivered to the reactor via Tylan Model FC-280 mass flow controllers and the reactor effluent composition was analyzed with a quadrapole mass spectrometer (UTI Model 100C). A mixture of N_2O in Ar (10.3 mol% N_2O Matheson) was diluted with 1 : 7 He. This mixture was passed over the catalyst at 0.10 MPa, and 363 K, at a total flow rate of 40 cm^3 (STP)/min. Exposed Cu surface areas were calculated assuming a reaction stoichiometry of two Cu atoms per oxygen atom and a Cu surface density of 1.46×10^{19} Cu atoms/m^2 (20, 21).

RESULTS

Activity Measurements

The compositions and designations of the catalysts used in this study are shown in Table 1. Also shown are the Cu surface areas determined by N_2O titration after reduction and after reaction (conditions described in following paragraph) for 5 h and subsequent re-reduction. The Cu surface area of Cu(5)Zr(0)Ti(0) and Cu(5)Zr(5)Ti(0) catalysts decreases after 5 h of reaction, while the Cu surface area of Cu(5)Zr(0)Ti(5) and Cu(5)Zr(2.5)Ti(2.5) catalysts increases. Reduced Cu(0)Zr(0)Ti(5) was tested to verify that TiO_2 does not react with N_2O. Others have found that ZrO_2 does not consume measurable quantities of N_2O (15).

The catalysts listed in Table 1 were reduced (see Experimental) and subsequently exposed to a mixture of H_2/CO_2 (3/1) at a total pressure of 0.65 MPa and a total flow of 60 cm^3 (STP)/min at 523 K for 4 h. Only the Cu-containing samples exhibited a measurable activity for methanol synthesis under these conditions. The results presented in Table 2 show that the addition of 5 wt% titania or zirconia to Cu/SiO_2 enhances the methanol synthesis activity. Increasing the titania loading from 5 to 30 wt% does not result in

TABLE 2

Effect of Catalyst on the Conversion of CO_2 to Methanol during CO_2 Hydrogenation[a]

Catalyst	Methanol activity (mol/s/g-cat)	Relative activity to Cu–SiO_2	Methanol selectivity (%)[b]
Cu(5)Zr(0)Ti(0)	1.0×10^{-7}	1.0	42
Cu(5)Zr(5)Ti(0)	1.5×10^{-7}	1.5	82
Cu(5)Zr(2.5)Ti(2.5)	4.5×10^{-7}	4.5	93
Cu(5)Zr(0)Ti(5)	1.8×10^{-7}	1.8	68
Cu(5)Zr(0)Ti(30)	1.8×10^{-7}	1.8	44

[a] Reaction conditions: $T = 523$ K: $P = 0.65$ MPa; $H_2/CO_2 = 3$; total flow rate = 60 cm^3 (STP)/min; total conversion <1%.

[b] The only other product is CO, formed by the reverse water–gas–shift reaction.

a further increase in activity, in contrast to earlier studies of the effects of ZrO_2 (15), which showed under reaction conditions identical to those used in the present study an increase in methanol synthesis activity by a factor of nine when the loading of ZrO_2 was increased from 5 to 30 wt%. The addition of both zirconia and titania to Cu/SiO_2 results in a catalyst with a higher methanol synthesis activity than when either zirconia or titania is added alone. Selectivity to methanol is also reported in Table 2. The only side reaction observed to occur was the reverse water–gas–shift reaction. Additions of oxides to Cu/SiO_2 increase the selectivity to methanol. Zirconia additions appear to be most effective at increasing the selectivity to methanol.

CO_2 Adsorption

Spectra of adsorbed CO_2 were taken by exposing the reduced samples to a CO_2/He mixture (1/3) flowing at 60 cm^3 (STP)/min and 0.65 MPa for 40 min at temperatures between 323 and 523 K. Figure 1 shows spectra collected at 373 K for the samples that do not contain copper. For Cu(0)Zr(0)Ti(5) the peak at 1600 cm^{-1} is due to bidentate bicarbonate on TiO_2 (*b*–HCO_3–Ti) (22, 23). For Cu(0)Zr(5)Ti(0) the peak at 1618 cm^{-1} is assigned to bidentate bicarbonate on ZrO_2 (*b*–HCO_3–Zr) (16, 24–32). The peak at 1608 cm^{-1} for Cu(0)Zr(2.5)Ti(2.5) is attributed to a combination of *b*–HCO_3–Ti and *b*–HCO_3–Zr. The other dominant feature seen for all samples is the peak at 1440 cm^{-1}, which is assigned to ionic carbonate species on either TiO_2 or ZrO_2 (*i*–CO_3–Zr/Ti) (16, 25–27, 32, 33). The shoulder observed at 1560 cm^{-1} in all cases is due to bidentate carbonate species on either TiO_2 or ZrO_2 metal oxide (*b*–CO_3–Zr/Ti) (16, 22, 24, 27, 29–33).

Figure 2a shows the total integrated area of the bicarbonate and carbonate peaks observed during CO_2 adsorption as a function of temperature. The total integrated area provides a measure of the surface concentrations of carbonates and bicarbonates assuming a constant extinction coefficient. For all catalysts the surface concentration of carbon-containing species decreases with increasing temperature, converging to a single value at 473 K. At low temperatures the Cu(0)Zr(2.5)Ti(2.5) sample has the highest surface concentration of carbonate and bicarbonate species and the lowest concentration of these species occurs on Cu(0)Zr(0)Ti(5). Shown in Fig. 2b are the peak intensities for the bidentate bicarbonate species adsorbed on the zirconia/titania. The data follow similar trends as observed in Fig. 2a.

Spectra taken during CO_2 adsorption at 373 K for the Cu-containing samples Cu(5)Zr(5)Ti(0), Cu(5)Zr(2.5)Ti(2.5), and Cu(5)Zr(0)Ti(5) are shown in Fig. 3. Compared to their counterparts, which do not contain Cu (see in Fig. 1), the relative intensities of the strongest features are about three times weaker. Ionic carbonate (*i*–CO_3–Ti) gives rise to the peak at 1431 cm^{-1} (33). The shoulder at 1441 cm^{-1} is indicative of *i*–CO_3–Zr (16, 25–27, 32). On Cu(5)Zr(5)Ti(0) peaks at 1617 and 1454 cm^{-1} represent *b*–HCO_3–Zr (16, 25–32). Also apparent are features for bidentate carbonate on titania (*b*–CO_3–Ti) at 1560–1540 and 1358 cm^{-1} (22, 32). The peaks at 1560–1540 and 1358 cm^{-1} are assigned to *b*–CO_3–Zr (25, 27, 31–33), whereas the features at 1521 and 1400–1380 cm^{-1} are assigned to monodentate carbonate on either titania (*m*–CO_3–Ti) (23, 33), or *m*–CO_3–Zr (16, 26,

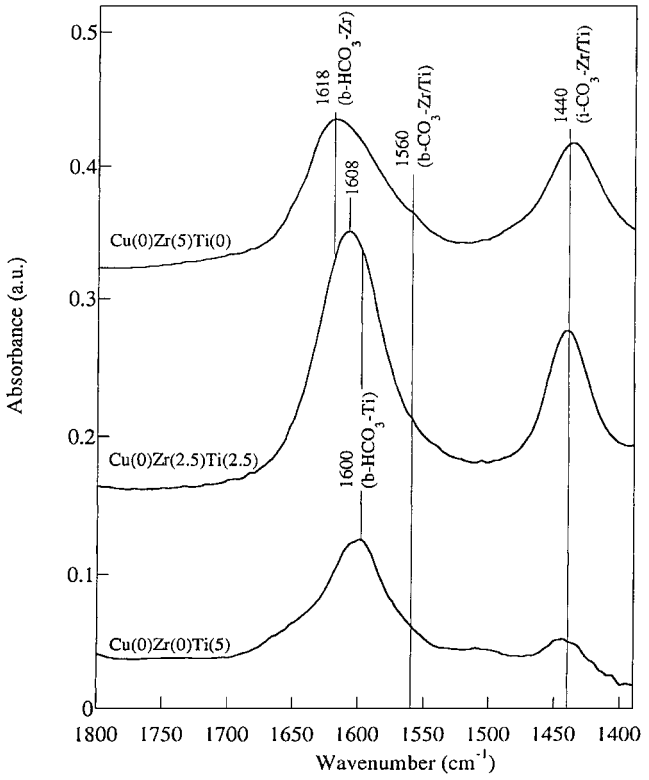

FIG. 1. Infrared spectra taken during exposure of Cu(0)Zr(5)Ti(0), Cu(0)Zr(2.5)Ti(2.5), and Cu(0)Zr(0)Ti(5) catalysts to 0.16 MPa CO_2 and 0.49 MPa He; total flow rate = 60 cm^3 (STP)/min; $T = 373$ K. Spectra referenced to each respective catalyst under 0.65 MPa He flow at 373 K.

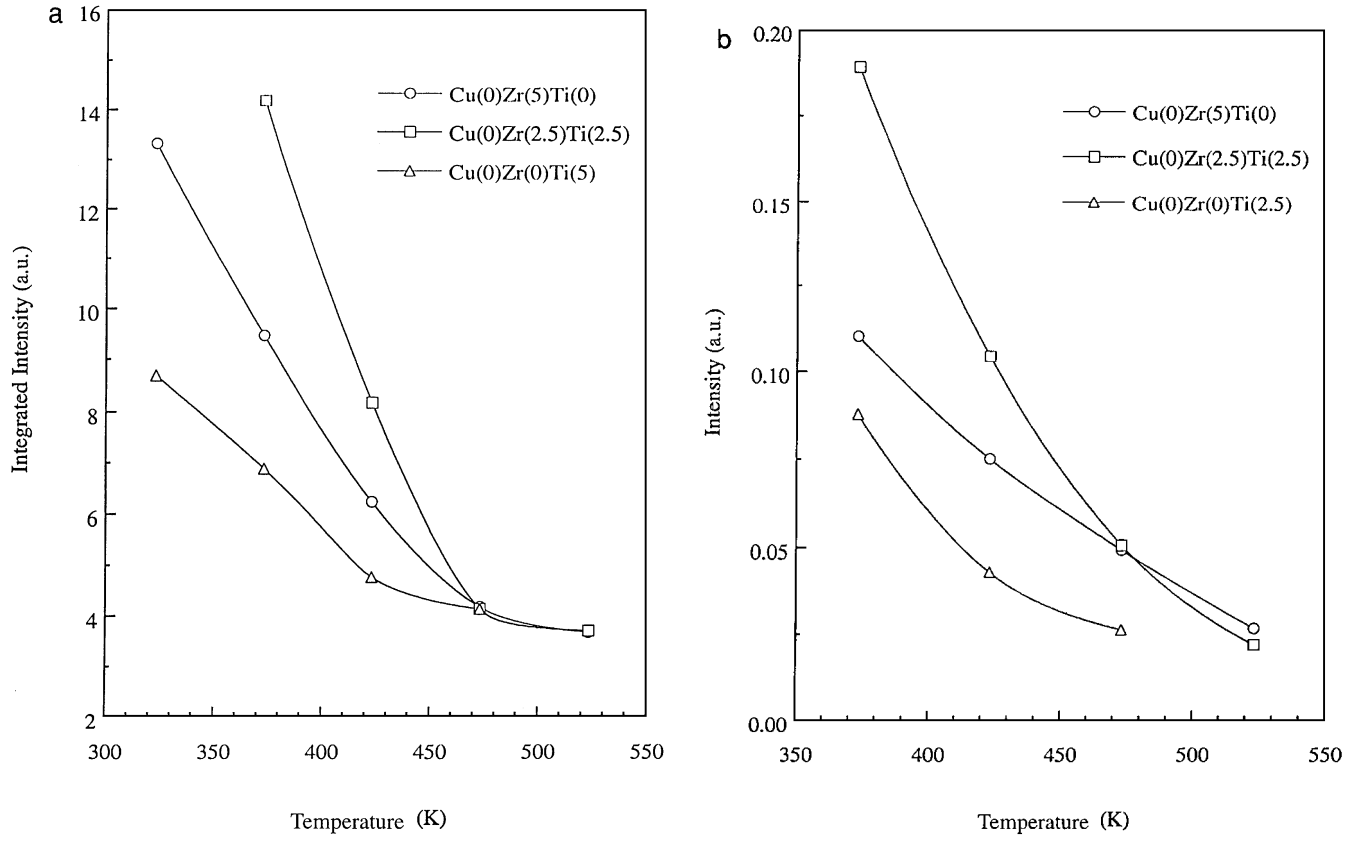

FIG. 2. (a) Total integrated area of carbonaceous species and intensity of *b*–HCO_3–Zr/Ti on Cu(0)Zr(5)Ti(0), Cu(0)Zr(2.5)Ti(2.5), and Cu(0)Zr(0)Ti(5) catalysts upon exposure to 0.16 MPa CO_2 and 0.49 MPa He; total flow rate = 60 cm^3 (STP)/min; $T = 323$–523 K. (b) Intensity of *b*–HCO_3–Zr/Ti (~1610 cm^{-1}) on Cu(0)Zr(5)Ti(0), Cu(0)Zr(2.5)Ti(2.5), and Cu(0)Zr(0)Ti(5) catalysts upon exposure to 0.16 MPa CO_2 and 0.49 MPa He; total flow rate = 60 cm^3 (STP)/min; $T = 357$–523 K.

27, 30, 32). The spectrum recorded for Cu(5)Zr(2.5)Ti(2.5) also displays features for *b*–HCO_3 (1617, 1454 cm^{-1}), *i*–CO_3 (1441 cm^{-1}), *m*–CO_3 (1521, 1400–1380 cm^{-1}), and *b*–CO_3 at (1560–1540, 1358 cm^{-1}). All of which are associated with either TiO_2 or ZrO_2. Additionally, bidentate formate on zirconia (*b*–HCOO–Zr) is observed, characterized by peaks at 2969 and 2892 (not shown), 1570, 1383, and 1365 cm^{-1} (16, 22, 28–31, 33–38).

Figure 4 shows the total integrated area of all carbon-containing species observed during CO_2 adsorption on the Cu-containing catalysts as a function of temperature. The total integrated area provides a measure of the surface concentrations of carbonates and bicarbonates assuming a constant extinction coefficient. As temperature increases, the amount of carbon-containing species decreases, converging to a single value for all catalysts at 523 K. Similar to what is observed in the absence of Cu, at temperatures below 523 K, the highest concentration of carbonaceous species is observed for Cu(5)Zr(2.5)Ti(2.5).

CO_2 Hydrogenation

Figure 5 shows spectra collected at 523 K in (STP)/min H_2/CO_2 (3/1), flowing at 60 cm^3, over reduced Cu(0)Zr(5)Ti(0), Cu(0)Zr(0)Ti(5), Cu(0)Zr(2.5)Ti(2.5), Cu(5)Zr(0)Ti(0), Cu(5)Zr(5)Ti(0), Cu(5)Zr(0)Ti(5), and Cu(5)Zr(2.5)Ti(2.5). The total system pressure in all cases was 0.65 MPa. Spectra were collected after 24 h exposure to the feed. Observable on all Cu-containing catalysts, except Cu(5)Zr(5)Ti(0), are features due to bidentate formate on Cu (*b*–HCOO–Cu) at 2930, 2850, 1539, and 1350 cm^{-1} (14, 16, 17, 39, 40). Methoxide species on silica (CH_3O–Si) are observed on all of the Cu-containing catalysts as evidenced by peaks at 2994, 2957, 2855, and 1463 cm^{-1} (16, 40–43). The zirconia-containing catalysts and Cu(0)Zr(0)Ti(5) exhibit features due to *b*–HCOO–Zr/Ti at 2972, 2900, 1574, 1389, and 1370 cm^{-1}. For the catalysts containing zirconia and Cu(0)Zr(0)Ti(5) methoxide species on zirconia/titania (CH_3O–Zr/Ti) are observed at 2937 and 2844 cm^{-1} (16, 28–31, 34, 37, 38, 44, 45).

Transient CO_2 Hydrogenation

Spectra were obtained after switching the feed from 3/1 He/CO_2 to 3/1 H_2/CO_2 at a total pressure of 0.65 MPa while maintaining the catalyst temperature at 523 K. The results shown in Fig. 6 for Cu(5)Zr(5)Ti(0) are qualitatively

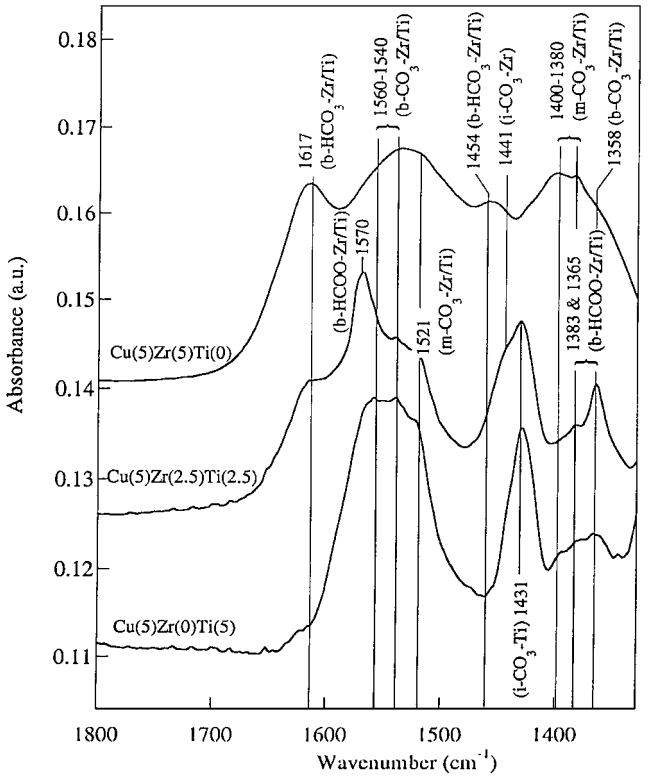

FIG. 3. Infrared spectra taken during exposure of Cu(5)Zr(5)Ti(0), Cu(5)Zr(2.5)Ti(2.5), and Cu(5)Zr(0)Ti(5) catalysts to 0.16 MPa CO_2 and 0.49 MPa He; total flow rate = 60 cm^3 (STP)/min; $T = 373$ K. Spectra referenced to each respective catalyst under 0.65 MPa He flow at 373 K.

similar to those obtained under the same conditions for $Cu/ZrO_2/SiO_2$ reported by Fisher *et al.* (16). At the beginning of the transient, *b*–HCO_3–Zr (1610 cm^{-1}), *b*–HCOO–Cu (2932, 2850, 1543, and 1350 cm^{-1}), and *b*–HCOO–Zr (2982, 2898, 1570, 1389, and 1370 cm^{-1}) are present. A peak for *b*–HCO_3–Zr is evident at the outset of the transient. This feature appears to increase slowly with time and is eventually overpowered by the large peak for *b*–HCOO–Zr (1570 cm^{-1}). Features due to formate on Cu (2932, 2850, 1543, and 1350 cm^{-1}) are eventually overlapped by more intense features due to CH_3O–Zr (2943 and 2846 cm^{-1}) and *b*–HCOO–Zr (1570, 1370 cm^{-1}). Formate features on zirconia increase rapidly initially, then plateau for the remainder of the 21-h transient. After about 1 min, features for CH_3O–Zr (2943 and 2846 cm^{-1}) appear and increase in intensity at longer times. After 1.2 min, features due to bidentate methylenebisoxy on zirconia (*b*–CH_2OO–Zr (2966 and 2861 cm^{-1})) (16, 28, 45–48) are present and features for CH_3O–Si (2959, 2856, and 1465 cm^{-1}) become observable and increase in intensity during the remainder of the transient.

Figure 7 shows spectra collected when the transient hydrogenation of CO_2 was carried out over Cu(5)Zr(0)Ti(5). These results are qualitatively similar to those obtained under the same conditions for Cu/SiO_2 (16). *b*–HCOO–Cu (2930, 2850, 1539, 1351 cm^{-1}) forms immediately upon switching from He/CO_2 to H_2/CO_2 and the intensities of the bands for this species remain relatively constant during the 25-h transient. After 3 min, a peak at 2958 cm^{-1} due to CH_3O–Si is observable and increases in intensity during the remainder of the transient. Companion peaks at 2995, 2856, and 1462 cm^{-1} become evident at longer times.

Spectra collected during the transient hydrogenation of CO_2 over Cu(5)Zr(2.5)Ti(2.5) are shown in Fig. 8. The key features of the catalyst are the rapid formation of *b*–HCOO–Cu (2933, 2849, 1540, and 1352 cm^{-1}) and the slower growth of CH_3O–Si (2992, 2957, 2856, and 1463 cm^{-1}). The growth of features due to *b*–HCOO–Zr (2900, 1570, 1387, and 1370 cm^{-1}) and to CH_3O–Zr (2937, 2839, and 1444 cm^{-1}) are clearly evident as is the presence of *b*–CH_2OO–Zr (2968 cm^{-1}).

Figure 9 shows the dynamics for the appearance of *b*–HCOO–Zr and CH_3O–Zr as determined by the growth in the intensities of the peaks at 1570 and 1444 cm^{-1}, respectively, for the experiments portrayed in Figs. 6 and 8. The peak at 1444 cm^{-1} was chosen as a measure of methoxide concentration, since the peaks at 2937 and 2839 cm^{-1} for CH_3O–Zr overlap the intense bands at 2933 and 2849 cm^{-1} for *b*–HCOO–Cu. The results from Fig. 7 are not shown since it is not possible to resolve the peaks for *b*–HCOO–Ti and *b*–CH_3O–Ti on Cu(5)Zr(0)Ti(5). In each case, the peak intensity has been normalized to the value observed at the end of the transient. It is evident that the initial rate of

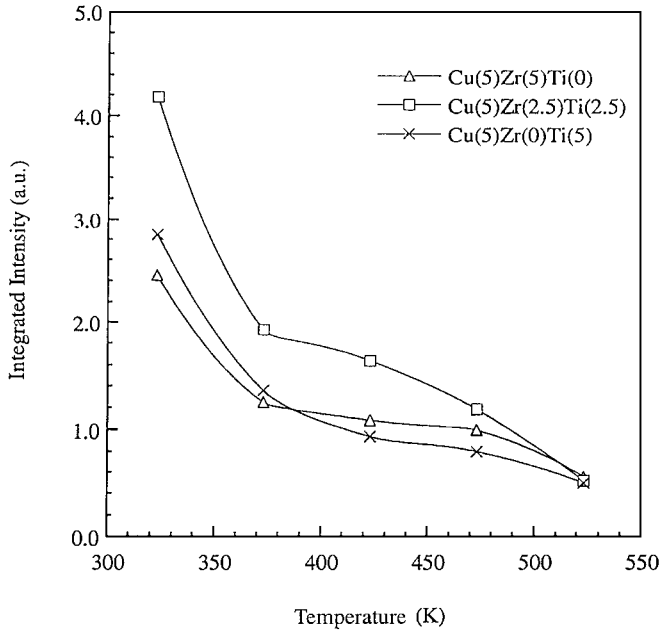

FIG. 4. Total integrated area of carbonaceous on Cu(5)Zr(5)Ti(0), Cu(5)Zr(2.5)Ti(2.5), and Cu(5)Zr(0)Ti(5) catalysts upon exposure to 0.16 MPa CO_2 and 0.49 MPa He; total flow rate = 60 cm^3 (STP)/min; $T = 323$–523 K.

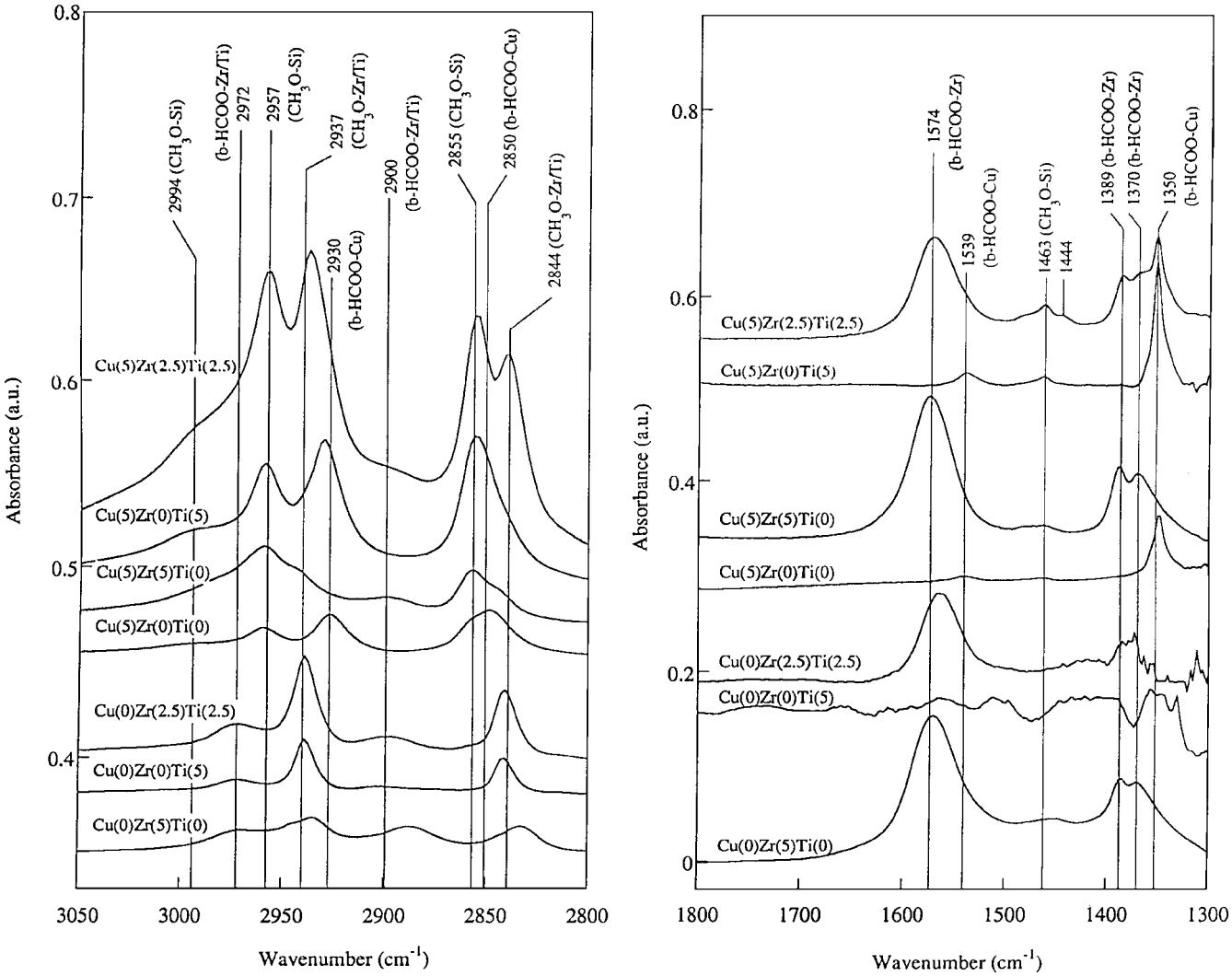

FIG. 5. Infrared spectra taken during exposure of Cu(0)Zr(5)Ti(0), Cu(0)Zr(0)Ti(5), Cu(0)Zr(2.5)Ti(2.5), Cu(5)Zr(0)Ti(0), Cu(5)Zr(5)Ti(0), Cu(5)Zr(0)Ti(5), and Cu(5)Zr(2.5)Ti(2.5) catalysts to 0.16 MPa CO_2 and 0.49 MPa H_2; total flow rate = 60 cm^3 (STP)/min; $T = 523$ K. Spectra referenced to each respective catalyst under 0.65 MPa H_2 flow at 523 K.

b–HCOO–Zr and CH_3O–Zr formation is similar for both catalysts. It is also apparent that the growth of methoxide is slower than that of the formate. Similar data were also collected for Cu(0)Zr(2.5)Ti(2.5). The growth of methoxide and formate peaks for this catalyst are too slow to be observable on the time scale depicted in Fig. 9, indicating that Cu is required for these species to form at an appreciable rate.

Transient Re-reduction in H_2

Spectra were obtained after switching the feed from 3/1 H_2/CO_2 to H_2 at a total pressure of 0.65 MPa while maintaining the temperature of the catalyst at 523 K. The results for Cu(5)Zr(5)Ti(0) are shown in Fig. 10. Features due to *b*–HCOO–Zr (2979, 2897, 1572, 1388, and 1368 cm^{-1}) decay most rapidly, whereas the features due to CH_3O–Si (2958 and 2857 cm^{-1}) and CH_3O–Zr (2943 and 2844 cm^{-1}) decay more slowly.

Figure 11 shows spectra taken during the reduction of Cu(5)Zr(0)Ti(5) and Cu(0)Zr(0)Ti(5) following the use of these catalysts for CO_2 hydrogenation. Under reducing conditions, Cu(5)Zr(0)Ti(5) behaves in the same manner as Cu(5)Zr(0)Ti(0) observed by Fisher *et al.* (16): features due to *b*–HCOO–Cu (2930, 2850, 1539, and 1352 cm^{-1}) decay rapidly and the CH_3O–Si species (2991, 2958, 2858, 1462 cm^{-1}) is more persistent. The *b*–HCOO–Ti features at 2970 and 2903 cm^{-1} disappear quite slowly on the Cu(0)Zr(0)Ti(5). For both catalysts features at 2939 and 2840 cm^{-1} are due to the presence of CH_3O–Ti. CH_3O–Ti species on Cu(5)Zr(0)Ti(5) are not a result of CO_2 hydrogenation on TiO_2. The lack of *b*–HCOO–Ti species on Cu(5)Zr(0)Ti(5), precursors to CH_3O–Ti, rule out this possibility.

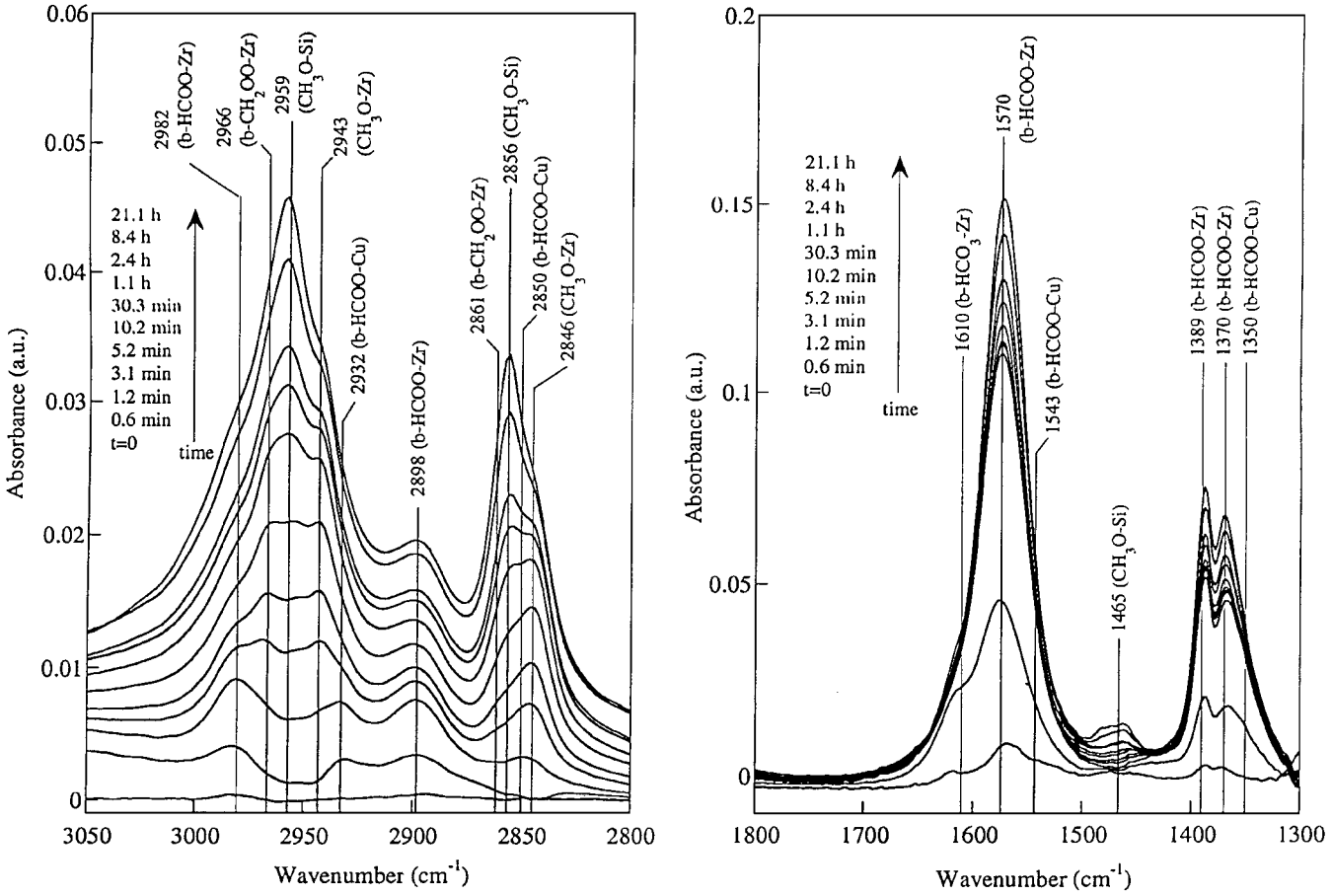

FIG. 6. Infrared spectra taken for Cu(5)Zr(5)Ti(0) at 523 K after switching feed from 0.16 MPa CO_2 and 0.49 MPa He to 0.16 MPa CO_2 and 0.49 MPa H_2; total flow rate = 60 cm^3 (STP)/min. Spectra referenced to Cu(5)Zr(5)Ti(0) under 0.65 MPa H_2 flow at 523 K.

The dynamics of reduction for species present on Cu(5)Zr(2.5)Ti(2.5) are shown in Fig. 12. The band due to *b*–HCOO–Cu (1352 cm^{-1}) decays rapidly; however, the decay of the companion peaks at 2931, 2855, and 1540 cm^{-1} cannot be tracked because these peaks overlap with larger features due to CH_3O–Zr (2943 cm^{-1}), CH_3O–Si (2856 cm^{-1}), and, *b*–HCOO–Zr (1570 cm^{-1}). *b*–HCOO–Zr (2900, 1570, 1387, and 1368 cm^{-1}) is also readily removed with H_2. The CH_3O–Zr species (2937, 2841, and 1444 cm^{-1}) decay slowly, whereas the CH_3O–Si species (2996, 2958, 2856, and 1463 cm^{-1}) are quite stable.

Figure 13 compares the dynamics of consumption of *b*–HCOO–Zr (1570 cm^{-1}) for Cu(5)Zr(5)Ti(0) and Cu(5)Zr(2.5)Ti(2.5) during the experiments shown in Figs. 10 and 12. Shown are the peak intensities normalized to their maximum intensities at the beginning of the transient. It is observed that formate hydrogenation occurs at the same rate for both catalysts. Similar data collected for Cu(0)Zr(2.5)Ti(2.5) show that formate hydrogenation occurs at an insignificant rate in the absence of Cu.

Figure 14 compares the dynamics of consumption of *b*–HCOO–Cu (1350 cm^{-1}) for Cu(5)Zr(0)/Ti(5), and Cu(5)Zr(2.5)/Ti(2.5). Data are also shown for Cu(5)Zr(0)/Ti(0) taken during an identical experiment reported by Fisher *et al.* (16). The peak intensities in each case have been normalized to their maximum intensities at the beginning of the transient. The result shows that Cu formate hydrogenation occurs at the same rate on all three catalysts.

Methoxide Hydrolysis

After the CO_2 hydrogenation reaction over Cu(5)Zr(2.5)Ti(2.5) and Cu(0)Zr(0)Ti(5) the feed was switched to H_2 at a pressure of 0.65 MPa flowing at 45 cm^3 (STP)/min, and the catalysts were reduced until only methoxide species were present in significant quantities ~72 h. The hydrolysis of the remaining CH_3O species (viz, $Zr–OCH_3 + H_2O \rightarrow Zr–OH + CH_3OH$) was investigated by switching the feed from H_2 to H_2 saturated with H_2O at 523 K. Shown in Fig. 15 are the methoxide peak intensities measured at 2841 cm^{-1}, normalized to their intensities observed before switching the feed from H_2 to H_2 saturated with H_2O. Included in this plot are data from Fisher *et al.* (16) for the same experiment on catalysts containing

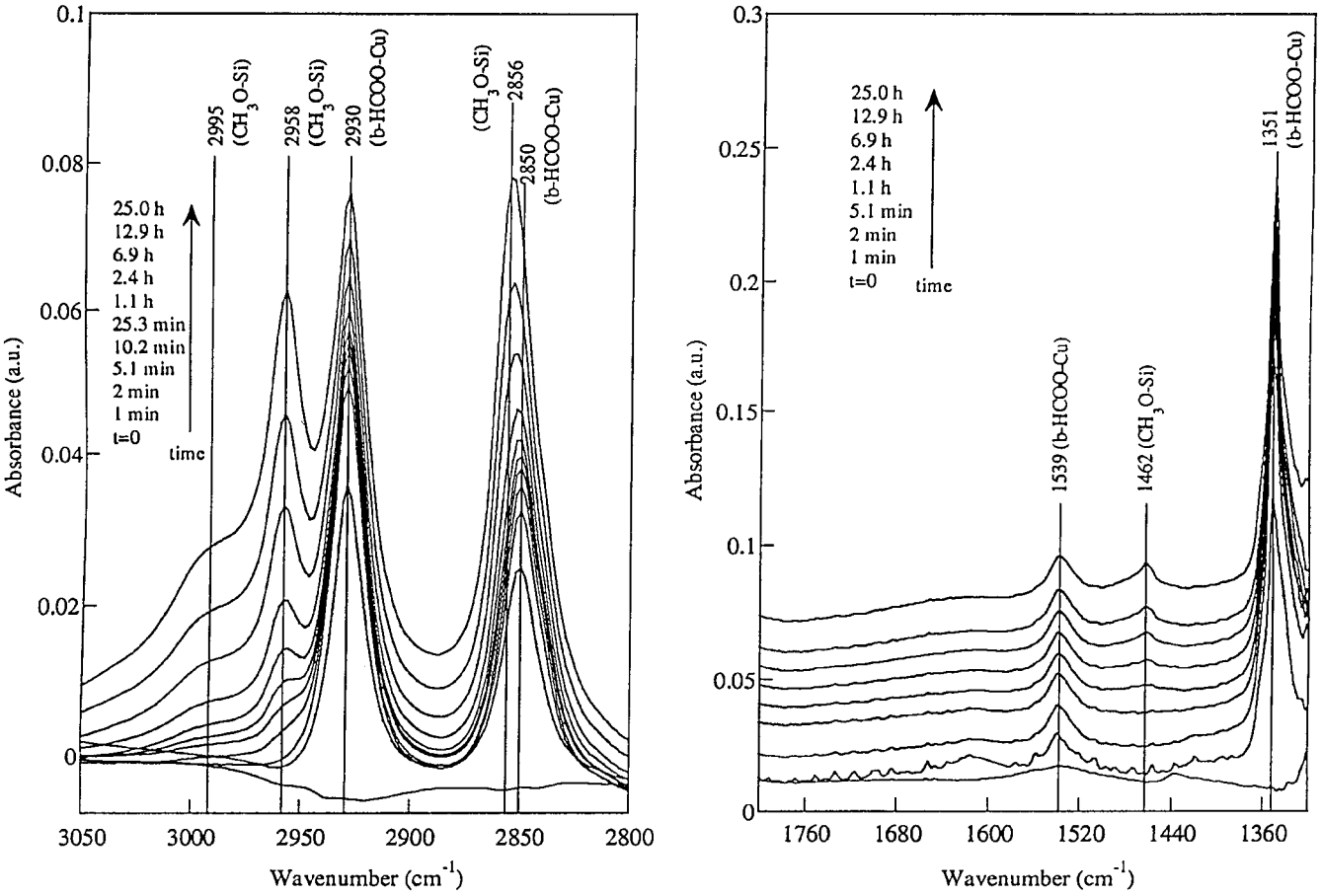

FIG. 7. Infrared spectra taken for Cu(5)Zr(0)Ti(5) at 523 K after switching feed from 0.16 MPa CO_2 and 0.49 MPa He to 0.16 MPa CO_2 and 0.49 MPa H_2; total flow rate = 60 cm^3 (STP)/min. Spectra referenced to Cu(5)Zr(0)Ti(5) under 0.65 MPa H_2 flow at 523 K.

zirconia (Cu(0)Zr(32)Ti(0), and Cu(5)Zr(31)Ti(0)). The results show that the methoxide species are hydrolyzed at the same rate on titania-containing catalysts as on catalysts containing zirconia.

DISCUSSION

It is clear from Table 2 that the addition of either TiO_2 or ZrO_2 increases the catalytic activity of Cu/SiO_2. It is also seen that the addition of both TiO_2 and ZrO_2 to Cu/SiO_2 results in a more active catalyst than when either TiO_2 or ZrO_2 alone is added to Cu/SiO_2. Moreover, the methanol synthesis activity increases with ZrO_2 loading (15), but not with TiO_2 loading. Therefore, the central issue is to understand how TiO_2 and ZrO_2, as well as their combination, affect methanol synthesis on $Cu–SiO_2$. An understanding of how these oxides impact methanol synthesis can be developed through a consideration of how each component affects this reaction.

Consistent with previous investigations (13, 16, 41, 42), it is observed that when Cu/SiO_2 is exposed to H_2/CO_2 the predominant species observed by infrared spectroscopy are *b*–HCOO–Cu and CH_3O–Si (see Fig. 5). Previous mechanistic studies conducted on this catalyst suggest that methanol synthesis over Cu proceeds via the stepwise hydrogenation of *b*–HCOO–Cu to form CH_2OO–Cu and CH_3O–Cu, the latter being the final precursor to methanol (16, 41, 42, 49). The presence of CH_3O–Si is attributed to the adsorption of gas-phase methanol by silica (16, 41, 42).

For the $Cu/ZrO_2/SiO_2$ catalyst, features due to *b*–HCOO–Cu demonstrate that methanol synthesis is occurring on Cu (see Fig. 6). However, for reaction times greater than 3 min the predominate species observed during CO_2 hydrogenation are HCOO–Zr, CH_2OO–Zr, and CH_3O–Zr (see Fig. 6). These observations are similar to those reported earlier for Cu(6)Zr(30)Ti(0) (16), for which it was demonstrated that methanol synthesis occurs via the hydrogenation of the carbonaceous species adsorbed on ZrO_2. The role of Cu is to adsorb H_2 dissociatively and supply atomic hydrogen to ZrO_2 by spillover (15, 16). For the chosen composition of the catalyst in this study, it is reasonable to

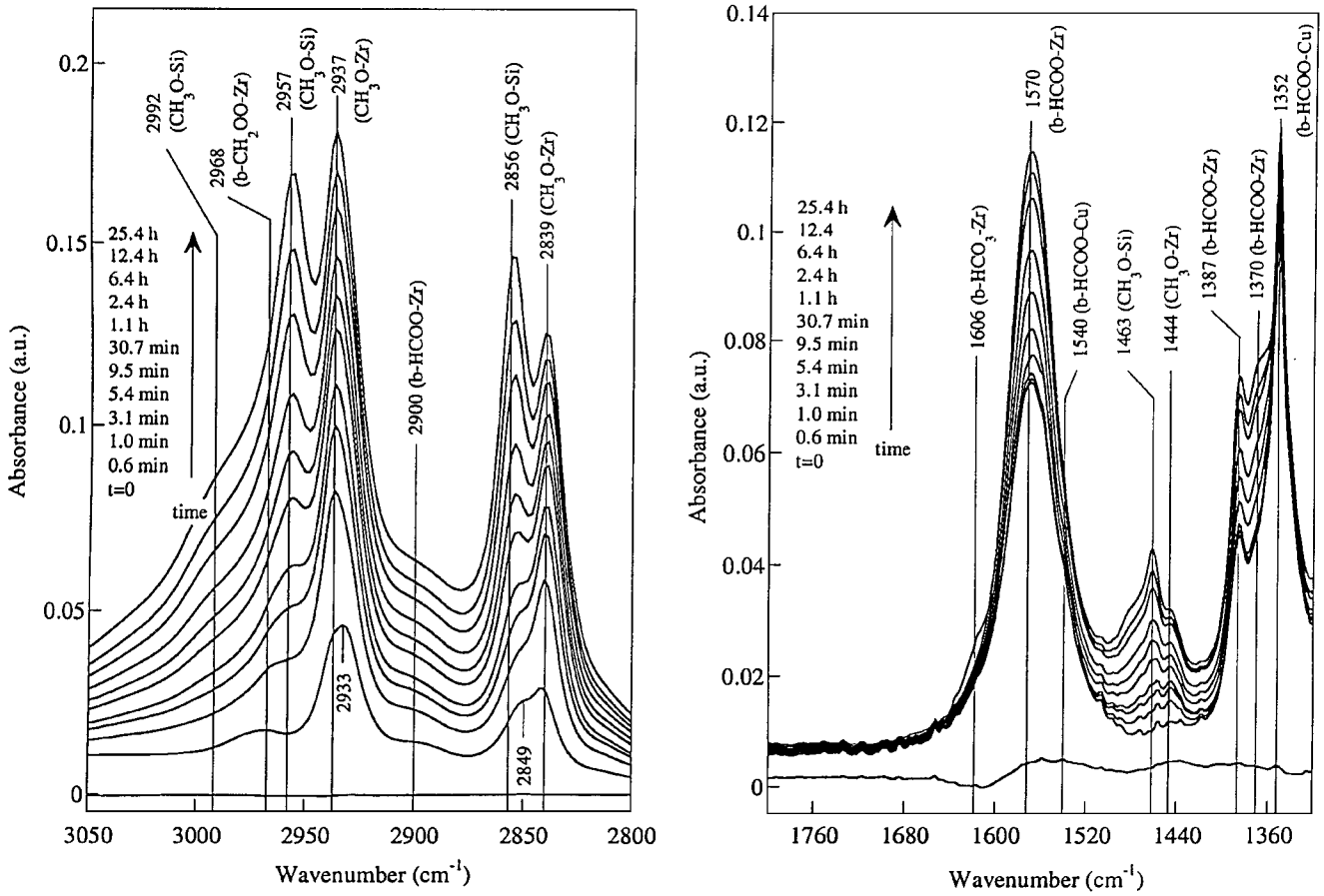

FIG. 8. Infrared spectra taken for Cu(5)Zr(2.5)Ti(2.5) at 523 K after switching feed from 0.16 MPa CO_2 and 0.49 MPa He to 0.16 MPa CO_2 and 0.49 MPa H_2; total flow rate = 60 cm^3 (STP)/min. Spectra referenced to Cu(5)Zr(2.5)Ti(2.5) under 0.65 MPa H_2 flow at 523 K.

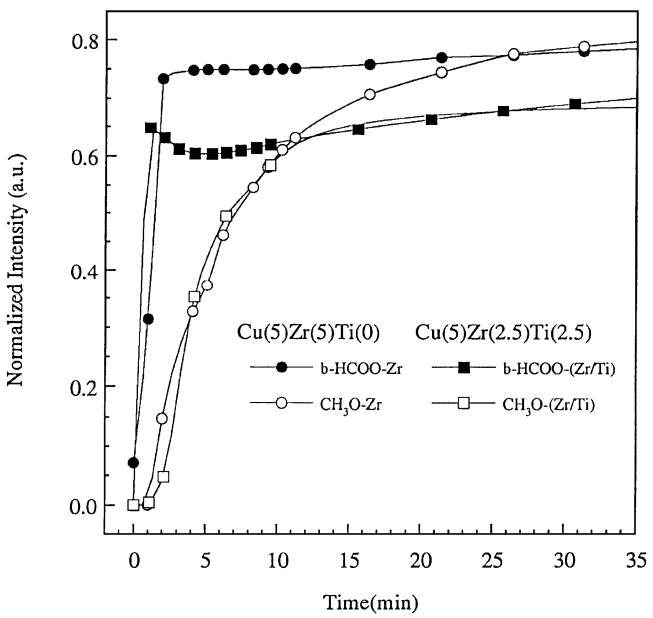

FIG. 9. Intensities of *b*–HCOO–Zr/Ti (~1570 cm^{-1}) and CH_3O–Zr/Ti (~1444 cm^{-1}) features for Cu(5)Zr(5)Ti(0) and Cu(5)Zr(2.5)Ti(2.5) during experiments in Figs. 7 and 9. Intensities normalized to those observed at the end of the transient.

conclude that methanol comes from both the Cu and the ZrO_2 components. With increased loadings of ZrO_2, the amount of methanol formed on the ZrO_2 component rises (16), and consistently the selectivity to methanol increases because the reverse water–gas–shift reaction occurs exclusively on the surface of Cu (15, 18).

The addition of TiO_2 to Cu/SiO_2 appears to enhance the synthesis of methanol from CO_2 by a mechanism that is different from that proposed to explain the effects of ZrO_2 addition. Two experimental observations suggest this to be the case. The first is that the addition of 5 and 30 wt% TiO_2 to Cu/SiO_2 have an identical effect on the rate of methanol synthesis (see Table 2). The second being that in strong contrast to Cu/ZrO_2/SiO_2, the dominant species observed under reaction conditions for Cu/TiO_2/SiO_2 is *b*–HCOO–Cu (see Figs. 5, 6, and 7), suggesting that upon addition of TiO_2, methanol synthesis continues to occur on Cu. Moreover, the intensity of *b*–HCOO–Cu is significantly higher for Cu/TiO_2/SiO_2 than for Cu/SiO_2 (see Fig. 5). Since the dispersion of Cu measured upon reduction of the used catalysts is not altered by addition of TiO_2 to Cu/SiO_2 (see Table 1) it is hard to argue that TiO_2 causes a significant increase in the dispersion of Cu. It is conceivable,

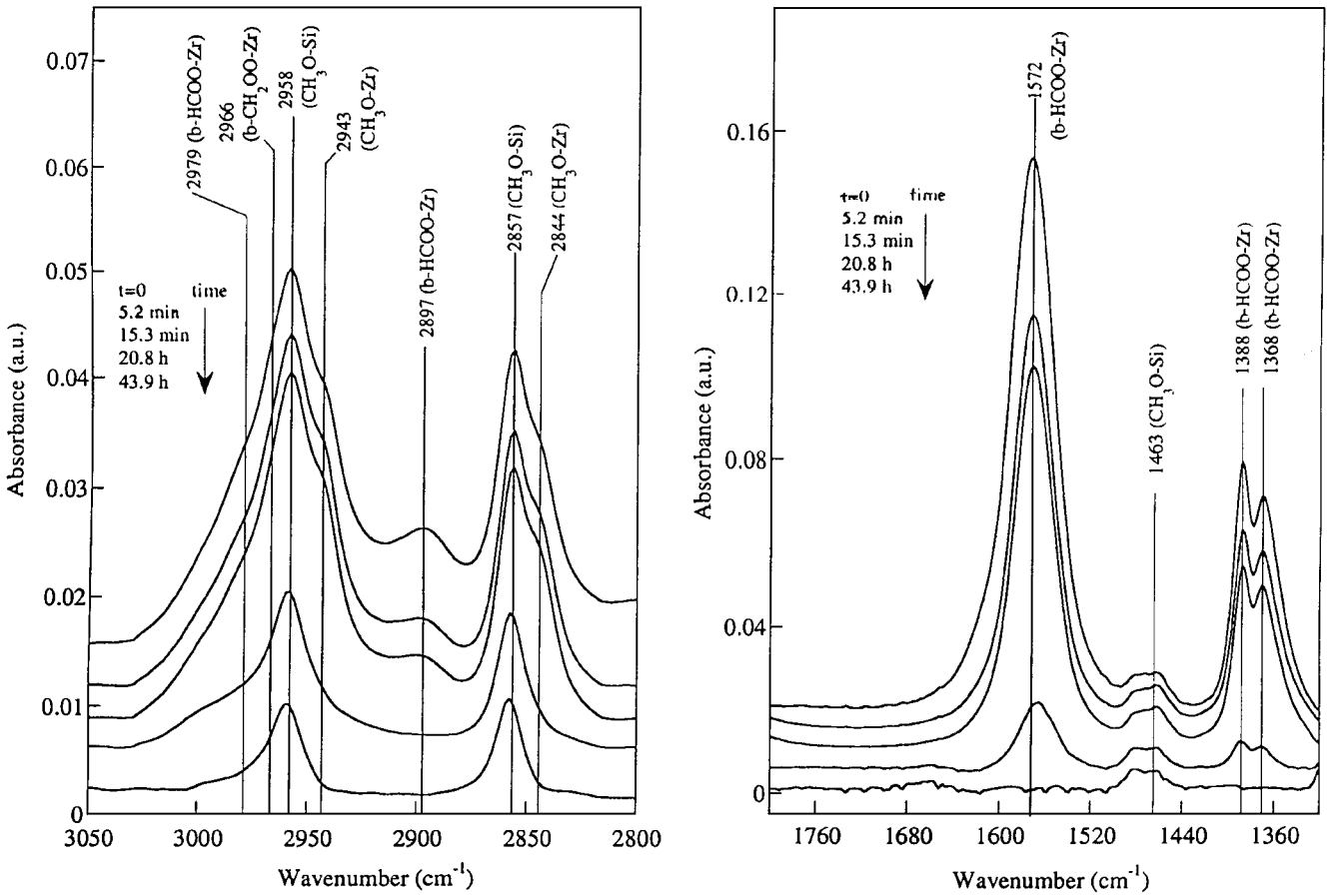

FIG. 10. Infrared spectra taken for Cu(5)Zr(5)Ti(0) at 523 K after switching feed from 0.16 MPa CO_2 and 0.49 MPa H_2 at a flow of 60 cm^3 (STP)/min to 0.65 MPa H_2 at a flow of 45 cm^3 (STP)/min. Spectra referenced to Cu(5)Zr(5)Ti(0) under 0.65 MPa H_2 flow at 523 K.

though, that TiO_2 causes a reconstruction of the dispersed Cu particles, particularly under reaction conditions, so that Cu (100) planes are exposed in preference to either (110) or (111) planes. Recent studies by Ovesen *et al.* (50) have shown that the rate parameter for the rate-limiting step in methanol synthesis over metallic Cu is 25 times higher over (100) surfaces than either the (110) or the (111) surfaces. Evidence for Cu reconstruction to exhibit Cu (100) surfaces preferentially has been found for Cu/ZnO catalysts (51).

The catalyst in which TiO_2 and ZrO_2 are added to Cu/SiO_2 exhibits the highest methanol synthesis activity from H_2/CO_2. The infrared spectra observed for $Cu/ZrO_2/TiO_2/SiO_2$ during reaction conditions appear to be a composite of those observed for $Cu/ZrO_2/SiO_2$ and $Cu/TiO_2/SiO_2$ (see Fig. 5). No evidence is observed for new species on the $Cu/ZrO_2/TiO_2/SiO_2$ catalyst. The spectra in Fig. 8 also show that there is simultaneous evolution of species on both ZrO_2 and Cu. The presence of Cu also serves to increase the rates of *b*–HCOO–Zr and CH_3O–Zr formation and elimination over those observed on $ZrO_2/TiO_2/SiO_2$ (see Results section of Figs. 9 and 13), again suggesting that Cu is involved in supplying atomic hydrogen for these processes. The surface concentration of Cu formate during CO_2 hydrogenation is observed to be higher for $Cu/ZrO_2/TiO_2/SiO_2$ than for Cu/SiO_2. Greater concentration of Cu formate is attributed to preferential reconstruction of more active Cu (100) surfaces under reaction, suggesting that methanol synthesis on the Cu component is being promoted in a similar manner to $Cu/TiO_2/SiO_2$. This evidence leads to the conclusion that the combination of TiO_2 and ZrO_2 to Cu/SiO_2 results in TiO_2 promotion of methanol synthesis on Cu, in addition to Cu promotion of methanol synthesis ZrO_2.

The present interpretation of the effects of TiO_2 additions and ZrO_2 and TiO_2 additions to Cu/SiO_2 differs from that proposed in Ref. (18). We had originally suggested that for all proportions of ZrO_2 and TiO_2 methanol synthesis occurred on the surface of the oxide and that the enhancement in methanol synthesis activity was due to variations in the concentration and strength of basic sites on the oxide surface. This interpretation was based on the observations of Tanabe *et al.* (52) who demonstrated a maximum in the concentration of basic sites with

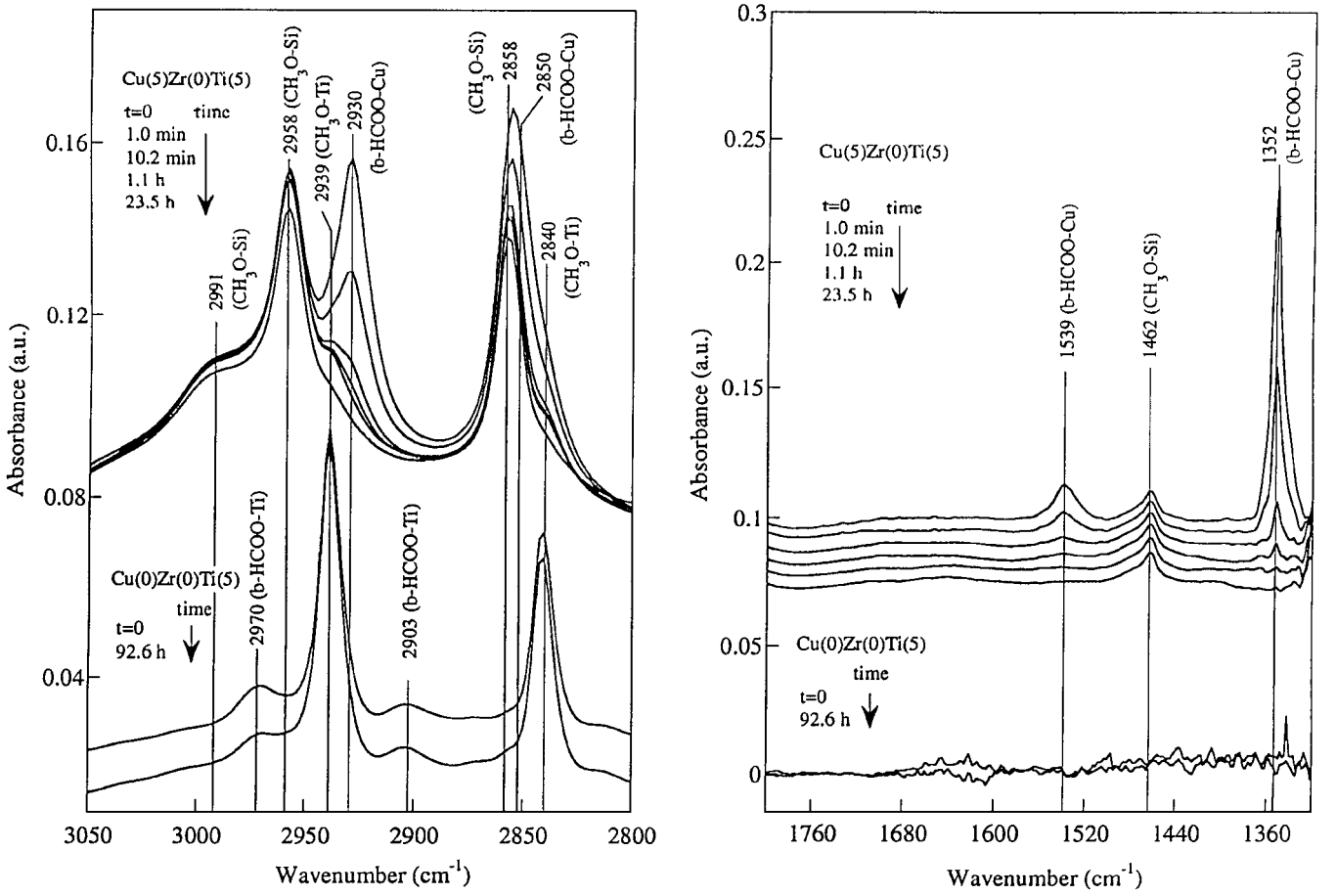

FIG. 11. Infrared spectra taken for Cu(5)Zr(0)Ti(5) and Cu(0)Zr(0)Ti(5) at 523 K after switching feed from 0.16 MPa CO_2 and 0.49 MPa H_2 at a flow of 60 cm^3 (STP)/min to 0.65 MPa H_2 at a flow of 45 cm^3 (STP)/min. Spectra referenced to Cu(5)Zr(0)Ti(5) and Cu(0)Zr(0)Ti(5), respectively under 0.65 MPa H_2 flow at 523 K.

variation in the proportions of ZrO_2 and TiO_2 in a mixed metal oxide. The results presented in Figs. 2a, 2b, and 4 show that for $T < 523$ K in fact, Cu(0)Zr(2.5)Ti(2.5) and Cu(5)Zr(2.5)Ti(2.5) adsorb CO_2 as HCO_3 and *i*-CO_3 to a significantly greater degree than materials containing either ZrO_2 or TiO_2 alone. However, the effects of combining ZrO_2 and TiO_2 on CO_2 adsorption diminish rapidly once the temperature is raised above 500 K, the temperature at which methanol synthesis becomes significant. At 523 K, Fig. 4 shows that the concentrations of carbonaceous species are the same on Cu(5)Zr(5)Ti(0), Cu(5)Zr(2.5)Ti(2.5), and Cu(5)Zr(0)Ti(5). As a consequence, the basicity of the mixed metal oxide appears not to be relevant for explaining the effects of TiO_2/ZrO_2 mixtures on the methanol synthesis activity of Cu/SiO_2.

CONCLUSIONS

For relatively small additions of ZrO_2 to Cu/SiO_2 *in situ* infrared spectroscopy shows that methanol synthesis occurs on both Cu and ZrO_2 components. Thus, the enhancement in activity of $Cu/ZrO_2/SiO_2$ over Cu/SiO_2 is due to a reaction occurring on both the zirconia and copper components. In contrast to what was observed for ZrO_2 additions, small additions of TiO_2 to Cu/SiO_2 do not alter the locus of methanol synthesis, which remains completely on the copper component. Experiments reveal that there is a greater surface concentration of Cu-formates on $Cu/TiO_2/SiO_2$. In this case the enhancement in activity of $Cu/TiO_2/SiO_2$ over Cu/SiO_2 is attributed to reconstruction of Cu (100) surface, under reaction conditions, which have been demonstrated to be significantly more active than (110) or (111) surfaces. The infrared spectra observed when a mixture of ZrO_2 and TiO_2 is added to Cu/SiO_2 resemble a composite of the spectra observed upon addition of the individual oxides, and hence, the enhanced rate of methanol synthesis is ascribed to the combined effects of ZrO_2 an TiO_2. In contrast to previous studies, acid–base interactions between CO_2 and metal oxides do not seem to fully account for the behavior of these catalysts during reaction conditions.

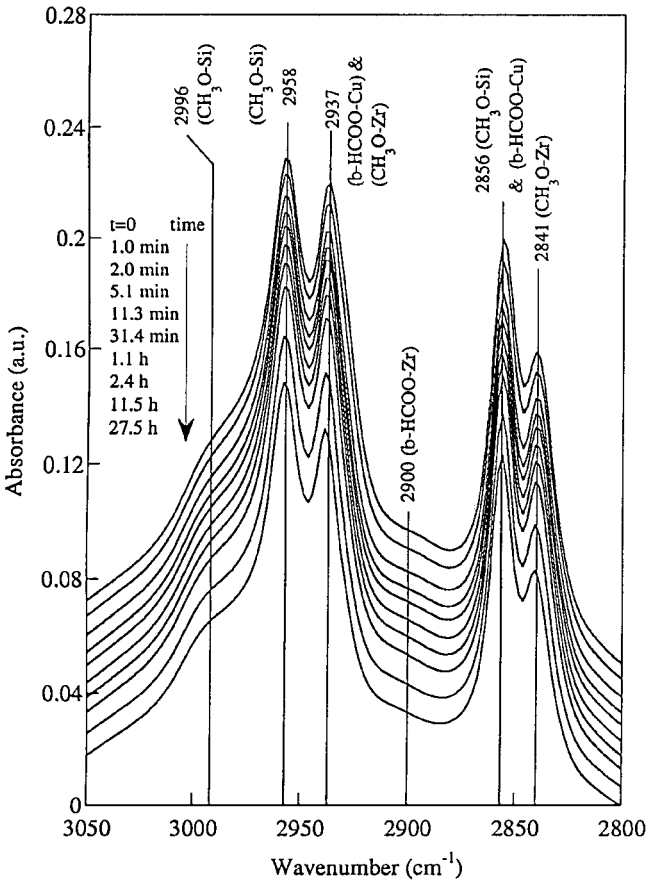

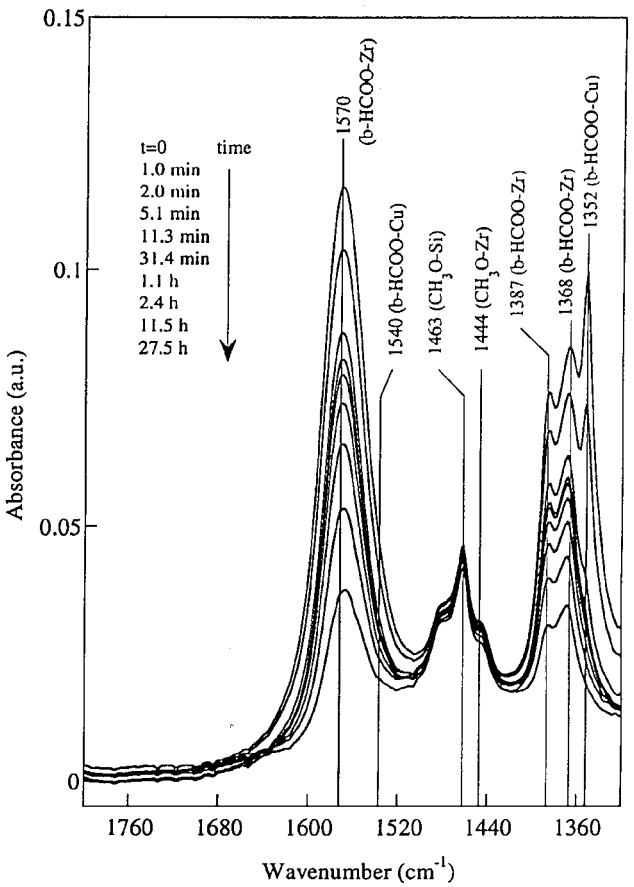

FIG. 12. Infrared spectra taken for Cu(5)Zr(2.5)Ti(2.5) at 523 K after switching feed from 0.16 MPa CO_2 and 0.49 MPa H_2 at a flow of 60 cm^3 (STP)/min to 0.65 MPa H_2 at a flow of 45 cm^3 (STP)/min. Spectra referenced to Cu(5)Zr(0)Ti(5) under 0.65 MPa H_2 flow at 523 K.

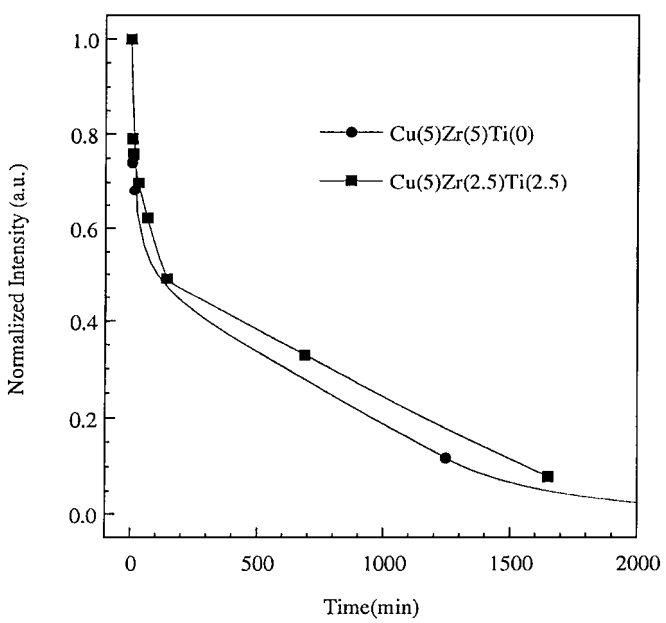

FIG. 13. Intensities of *b*–HCOO–Zr/Ti (1570 cm^{-1}) features for Cu(5)Zr(5)Ti(0) and Cu(5)Zr(2.5)Ti(2.5) during experiments in Figs. 10 and 12. Intensities normalized to those observed at the beginning of the transient.

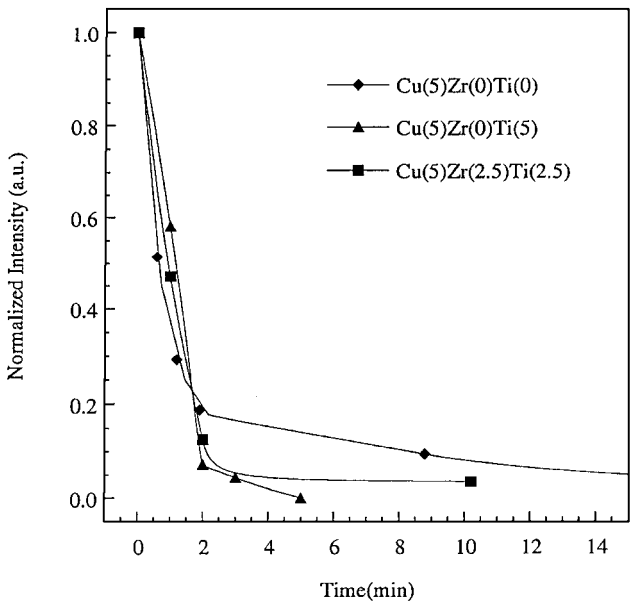

FIG. 14. Intensities of *b*–HCOO–Cu (1350 cm^{-1}) features for Cu(5)Zr(0)Ti(0), Cu(5)Zr(0)Ti(5), and Cu(5)Zr(2.5)Ti(2.5) catalysts during experiments in Figs. 11 and 12. Intensities normalized to those observed at the beginning of the transient. Data for Cu(5)Zr(0)Ti(0) was taken from Fisher *et al.* (16).

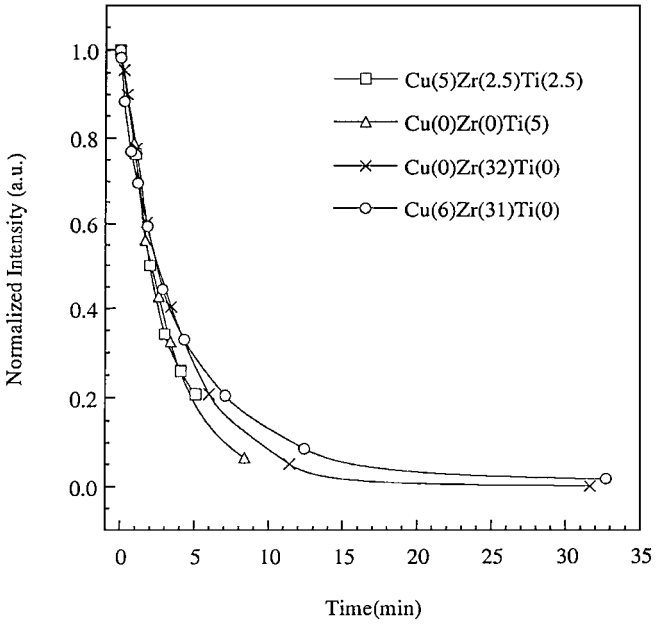

FIG. 15. Intensities of CH_3O–Zr/Ti (2841 cm^{-1}) features for Cu(5)Zr(2.5)Ti(2.5), Cu(0)Zr(0)Ti(5), Cu(0)Zr(32)Ti(0), and Cu(6)Zr(31)Ti(0) catalysts after switching feed from 0.10 MPa H_2 to H_2O saturated ($PH_2O = 3.2$ kPa) H_2 at total pressure of 0.10 MPa at a flow of 60 cm^3 (STP)/min at 523 K. Intensities normalized to those observed at the beginning of the transient. Data for Cu(0)Zr(32)Ti(0), and Cu(6)Zr(31)Ti(0) were taken from Fisher *et al.* (16).

ACKNOWLEDGMENTS

This work was supported by the Director, Office of Basic Energy Sciences, Chemical Sciences Division, of the U.S. Department of Energy under Contract DE-AC03-76SF00098.

REFERENCES

1. Highfield, J. G., *Trends Phys. Chem.* **5**, 91 (1995).
2. Klier, K., *Adv. Catal.* **31**, 243 (1982).
3. Bartley, G. J. J., and Burch, R., *Appl. Catal.* **43**, 141 (1988).
4. Robinson, W. R. A. M., and Mol, J. C., *Appl. Catal.* **44**, 165 (1988).
5. Denise, B., and Sneeden, R. P. A., *Appl. Catal.* **28**, 235 (1986).
6. Chen, H. W., White, J. M., and Ekerdt, J. G., *J. Catal.* **99**, 293 (1986).
7. Amenomiya, Y., *Appl. Catal.* **30**, 57 (1987).
8. Denise, B., Sneeden, R. P. A., Beguin, B., and Cherifi, O., *Appl. Catal.* **30**, 353 (1987).
9. Bartley, G. J. J., and Burch, R., *Appl. Catal.* **43**, 141 (1988).
10. Kanoun, N., Astier, M. P., and Pajonk, G. M., *Catal. Lett.* **15**, 231 (1992).
11. Koeppel, R. A., Baiker A., and Wokaun, A., *Appl. Catal. A* **84**, 77 (1992).
12. Sun, Y., and Sermon, P. A., *J. Chem. Soc., Chem. Commun.*, 1242 (1993).
13. Nitta, Y., Suwata, O., Ikeda, Y., Okamoto, Y., and Imanaka, T., *Catal. Lett.* **26**, 345 (1994).
14. Tagawa, T., Nomura, N., Shimakage, and Goto, M., S., *Res. Chem. Intermed.* **21**, 193 (1995).
15. Fisher, I. A., Woo, H. C., and Bell, A. T., *Catal. Lett.* **44**, 11 (1997).
16. Fisher, I. A., and Bell, A. T., *J. Catal.* **172**, 222 (1997).
17. Nomura, N., Tagawa, T., and Goto, M., *Appl. Catal. A* **166**, 321 (1998).
18. Schilke, T. C., Fisher, I. A., and Bell, A. T., *Catal. Lett.* **54**, 105 (1998).
19. Hicks, R. F., Kellner, C. S., Savatsky, B. J., Hecker, W. C., and Bell, A. T., *J. Catal.* **71**, 216 (1981).
20. Scholten, J. J., and Konvalinka, J. A., *J. Chem. Soc. Faraday Trans.* **65**, 24 (1969).
21. Chinchen, G. C., Hay, C. M., Vandervell, H. D., and Waugh, K. C., *J. Catal.* **79**, 103 (1987).
22. Rethwisch, D. G., and Dumesic, J. A., *Langmuir* **2**, 73 (1986).
23. Morterra, C., Chiorino, A., Boccuzzi, F., and Fisicaro, E., *Z. Physik. Chem. Neue Folge* **124**, 211 (1981).
24. Tret`yakov, N. E., Pozdnyakov, D. V., Oranskaya, O. M., and Filimonov, V. N., *Russ. J. Phys. Chem.* **44**, 596 (1970).
25. Bianchi, D., Chafik, T., Khalfallah, M., and Teicher, S., *J. Appl. Catal. A* **112**, 57 (1994).
26. Bianchi, D., Chafik, T., Khalfallah, M., and Teicher, S., *J. Appl. Catal. A* **112**, 219 (1994).
27. Chafik, T., Bianchi, D., Khalfallah, M., and Teicher, S., *Topics in Catal.* **2**, 103 (1995).
28. He, M. Y., and Ekerdt, J. G., *J. Catal.* **87**, 381 (1984).
29. Kondo, J., Abe, H., Sakata, Y., Maruya, K., Domen, K., and Onishi, T., *J. Chem. Soc. Faraday Trans.* **184**, 511 (1988).
30. Hertl, W., *Langmuir* **5**, 96 (1989).
31. Guglielminotti, E., *Langmuir* **6**, 1455 (1990).
32. Morterra, C., and Orio, L., *Mat. Chem. Phys.* **24**, 247 (1990).
33. Mascetti, J., and Tranquile, M., *J. Phys. Chem.* **92**, 2177 (1988).
34. Weigel, J., Koeppel, R. A., Kaiker, A., and Wokaun, A., *Langmuir* **12**, 5319 (1996).
35. Bianchi, D., Chafik, T., Khalfallah, M., and Teicher, S., *J. Appl. Catal. A* **105**, 223 (1993).
36. He, M. Y., and Ekerdt, J. G., *J. Catal.* **90**, 17 (1984).
37. Hussein, G. A., Sheppard, N., Zaki, M. I., and Fahim, R. B., *J. Chem. Soc. Faraday Trans.* **87**, 2655 (1991).
38. Suda, Y., Morimoto, T., and Nagao, M., *Langmuir* **3**, 99 (1987).
39. Millar, G. J., Rochester, C. H., and Waugh, K. C., *J. Chem. Soc. Faraday Trans.* **87**, 1491 (1991).
40. Millar, G. J., Rochester, C. H., and Waugh, K. C., *J. Chem. Soc. Faraday Trans.* **87**, 2795 (1991).
41. Clarke, D. B., Lee, D. K., Sandoval, M. J., and Bell, A. T., *J. Catal.* **150**, 81 (1994).
42. Clarke, D. B., and Bell, A. T., *J. Catal.* **154**, 314 (1995).
43. Wovchko, E. A., Camp, J. C., Glass, J. A., and Yates, J. T., *Langmuir* **11**, 2592 (1995).
44. Carrizosa, I., Munuera, G., and Castanar, S., *J. Catal.* **49**, 265 (1977).
45. Lavalley, J., Lamotte, J., Busca, G., and Lorenzelli, V., *J. Chem. Soc. Chem. Commun.*, 1006 (1985).
46. Stuve, E. M., Madix, R. J., and Sexton, B. A., *Surf. Sci.* **119**, 279 (1982).
47. Onishi, T., Abe, H., Maruya, K., and Domen, K., *J. Chem. Soc. Chem. Commun.*, 103 (1986).
48. Idriss, K., Hindermann, J. P., Kieffer, R., Kiennemann, A., Vallet, A., Chauvin, C., Lavalley, J. C., and Chaumette, P., *J. Mol. Catal.* **42**, 205 (1987).
49. Askgaard, T. S., Nørskov, J. K., Ovesen, C. V., and Stoltze, P., *J. Catal.* **156**, 229 (1995).
50. Ovesen, C. V., Clausen, B. S., Schiøtz, J., Stoltze, P., Topsøe, H., Nørskov, J. K., *J. Catal.* **168**, 133 (1997).
51. Clausen, B. S., Shiøtz, J., Grabaek, L., Ovesen, C. V., Jacobsen, K. W., Nørskov, J. K., Topsøe, H., *Top. Catal.* **1**, 367 (1994).
52. Arata, K., Akutagawa, S., and Tanabe, K., *Bull. Chem. Soc. Japan.* **49**, 390 (1976).